Cell

Rab and Arl GTPase Family Members Cooperate in the Localization of the Golgin GCC185

Alondra Schweizer Burguete,[1,2] Timothy D. Fenn,[2] Axel T. Brunger,[2] and Suzanne R. Pfeffer[1,*]
[1]Department of Biochemistry
[2]Howard Hughes Medical Institute, Departments of Molecular and Cellular Physiology, Neurology, Structural Biology and Photon Science
Stanford University School of Medicine, Stanford, CA 94305 USA
*Correspondence: pfeffer@stanford.edu
DOI 10.1016/j.cell.2007.11.048

SUMMARY

GCC185 is a large coiled-coil protein at the trans Golgi network that is required for receipt of transport vesicles inbound from late endosomes and for anchoring noncentrosomal microtubules that emanate from the Golgi. Here, we demonstrate that recruitment of GCC185 to the Golgi is mediated by two Golgi-localized small GTPases of the Rab and Arl families. GCC185 binds Rab6, and mutation of residues needed for Rab binding abolishes Golgi localization. The crystal structure of Rab6 bound to the GCC185 Rab-binding domain reveals that Rab6 recognizes a two-fold symmetric surface on a coiled coil immediately adjacent to a C-terminal GRIP domain. Unexpectedly, Rab6 binding promotes association of Arl1 with the GRIP domain. We present a structure-derived model for dual GTPase membrane attachment that highlights the potential ability of Rab GTPases to reach binding partners at a significant distance from the membrane via their unstructured and membrane-anchored, hypervariable domains.

INTRODUCTION

Vesicle-mediated transport between membrane bound compartments is essential for protein secretion, cell signaling and cell growth. Transport involves the collection of specific cargo molecules into vesicles, movement of vesicles by motors along cytoskeletal tracks, and tethering, docking and fusion of vesicles at the target membrane (Pfeffer, 1999). GTPases of the Rab and Arf families play central roles in the regulation of these processes by recruiting specific partner ("effector") proteins to the membranes upon which they are bound (Grosshans et al., 2006; Gillingham and Munro, 2007). The GTPases interconvert between active, GTP bound forms that are capable of effector interactions, and inactive, GDP-bound forms; interconversion is catalyzed by GTPase-specific enzymes.

Among GTPase effectors are proteins that have been demonstrated to function as transport vesicle tethers. Tethers function to bring partner membranes into close proximity before membrane fusion (Sztul and Lupashin, 2006). One class is comprised of macromolecular assemblies such as the Exocyst and TRAPP complexes; another class is comprised of large coiled-coil proteins such as p115 and EEA1 (Sztul and Lupashin, 2006). GCC185 is a putative coiled-coil tether of 185 kDa that belongs to the Golgi-localized Golgin family of proteins. GCC185 is required for Rab9-dependent transport of mannose 6-phosphate receptors from late endosomes to the trans-Golgi network (TGN; Reddy et al., 2006; Derby et al., 2007). In support of the notion that this protein functions as a tether, cells depleted of GCC185 accumulate their cargo in peripheral, Rab9-positive vesicles (Reddy et al., 2006). A recent study demonstrated that GCC185 is also required for the attachment of noncentrosomal microtubules to the TGN via CLASPs, proteins that stabilize microtubule plus ends and prolong their elongation from the TGN (Efimov et al., 2007). Since GCC185 is a key player in both membrane traffic and cytoskeletal organization, it is important to determine how GCC185 is localized to the TGN.

GCC185 is one of four human Golgins (Golgin-245, Golgin-97, GCC88, and GCC185) that contain a GRIP domain. The ~45 residue GRIP domain represents an Arl1 GTPase-binding unit and is sufficient to specify Golgi-targeting of Golgin-97 and Golgin-245 via Arl1 binding (Gillingham and Munro, 2007). The crystal structure of Arl1 bound to the Golgin-245 GRIP domain has been determined (Panic et al., 2003; Wu et al., 2004) and confirmed the importance of an invariant GRIP domain tyrosine residue for Arl1 binding and Golgi localization of Golgin-245 and Golgin-97. Surprisingly, despite its relatively well conserved GRIP domain, we and others found that GCC185 binds very poorly to Arl1, and mutation of the invariant GRIP domain tyrosine residue interfered only weakly with GCC185's Golgi localization (Lu and Hong, 2003; Derby et al., 2004; Reddy et al., 2006). GCC185 differs from other GRIP domain proteins in its TGN sub-localization (Luke et al., 2003; Derby et al., 2004). In addition, attempts to re-localize GCC185 in cells expressing an early endosome-targeted Arl1 were not successful, despite efficient re-localization of Golgin-97 and Golgin-245 (Derby et al., 2004). Together, these data suggested that GCC185 is localized to the TGN by

a mechanism that is distinct from that used by Golgin-245 and Golgin-97.

In this study we define an independent Rab GTPase-binding site near the C terminus of GCC185. We show that Rab6 binds to this site and we present the three dimensional crystal structure of the Rab6:Rab-binding domain complex. Analysis of mutant proteins revealed that the Rab-binding domain regulates both Golgi association and Arl1 binding to the GCC185 GRIP domain. Thus, two members of distinct GTPase families cooperate to localize GCC185 to the Golgi.

RESULTS

We tested the Golgi associated, Rab6 GTPase for its possible interaction with GCC185. Rab6 was an obvious candidate, as it localizes to the Golgi and both yeast (Ypt6p) and human proteins interact with several putative tethering proteins, including the yeast VFT/GARP complex (Siniossoglou and Pelham, 2001), and the yeast protein Sgm1 and its mammalian homolog, TMF (Fridmann-Sirkis et al., 2004). In addition, there is strong genetic interaction between the genes encoding Ypt6p and the sole, yeast GRIP domain protein, Imh1p (Li and Warner, 1996; Tsukada and Gallwitz, 1996).

For these experiments, a construct of GST fused to the GCC185 C terminus was employed that includes a ~45 residue GRIP domain, plus ~40 amino acids upstream of this domain and ~20 amino acids that extend to the C terminus (C-110; Figure 1A). As shown in Figure 1B (left panel), C-110 bound Rab6-GTP with a 5-fold preference over Rab6-GDP, which defines GCC185 as a Rab6 effector. This interaction was specific in that the C-110 fragment did not bind Rab1 (Figure 1C), Rab5 (Reddy et al., 2006) or Arl1-GTP (Figure 1C) at comparable concentrations. However Arl1 binding is observed when a higher (approximately 3-fold) C-110 concentration is used (see below). A somewhat larger, 158 residue construct did not yield a higher bound fraction of Rab6 protein (data not shown), demonstrating that an entire Rab-binding site lies within the 110 C-terminal residues of GCC185.

A specific, conserved GRIP domain tyrosine residue was previously shown to be critical for Arl1-binding and Golgi recruitment of Golgin-245 and Golgin-97 (Barr, 1999; Kjer-Nielsen et al., 1999). Mutation of the corresponding tyrosine residue in GCC185 (Y1618A) had no influence on Rab6 (Figure 1C) or Rab9 binding (Reddy et al., 2006; Figure 1C), consistent with a different mode of interaction for Rabs with GCC185. As a construct comprised of the 72 C-terminal residues of GCC185 (C-72; Figure 1A) failed to bind Rab6 or Rab9 (Figure 1C), we conclude that the GRIP domain is dispensible for Rab binding.

Residues just upstream of the GRIP domain (1575–1613; RBD in Figure 1A) comprise a Rab-binding domain. As shown in Figure 1B (right panel), the so-called RBD-87 polypeptide that includes this region but lacks the GRIP domain was sufficient for full Rab6 binding. In contrast, the RBD-87 construct bound only about 25% of Rab9 as compared to C-110 (Figure 1B, right panel), suggesting that Rab9 interacts at least in part with the GRIP domain. Interestingly, Rab6 and Rab9 C-terminal hypervariable domains contributed to GCC185 binding, as a chimeric Rab9 protein containing the hypervariable domain of Rab1 (Rab9/1; Aivazian et al., 2006) or a Rab6 construct lacking the hypervariable domain (Rab6 1–174) failed to bind C-110 (Figure 1C). Thus, residues 1575–1613 comprise a region in GCC185 that is necessary for Rab binding, and additional downstream sequences are needed for Rab9 but not Rab6.

An anti-Rab9 immunoblot-based binding assay was used to test whether Rab6 and Rab9 compete for interaction with GCC185. Briefly, the C-110 fragment was incubated with Rab9, either alone or with excess Rab6 or Rab1. When a 10-fold excess Rab6 competitor was added to the preformed Rab9-GCC185 complex, Rab9 binding was reduced to background levels (Figure 1D, upper panel; compare lanes 7 and 8 with 5 and 6). An equal amount of Rab6 competitor decreased the Rab9-bound fraction to 50% (data not shown). In contrast, a ten-fold excess of Rab1 did not compete with Rab9 for GCC185 binding (Figure 1D, lanes 9 and 10). In addition, Rab9 could compete for Rab6 binding, although it was a less potent competitor (Figure 1D, lower panel). Thus, Rab6 and Rab9 compete for GCC185 binding both specifically and efficiently. Together, these data confirm that Rab6 and Rab9 bind to at least partially overlapping sites on GCC185.

The binding affinities for GCC185 with Rab6 and Rab9 were determined by isothermal titration calorimetry. Figures S1A and S1B (available online) show representative, isothermal titration calorimetric (ITC) raw data for nucleotide-preloaded, Rab6-GTP and Rab9-GTP upon injection into a cell containing GST-C-110 (upper panels). Peak size was diminished with each injection as the binding reaction reached saturation. As expected, titrations of Rab6-GTP and Rab9-GTP into buffer (upper-panel insets) or into GST (lower panel insets) resulted in heats comparable to baseline values in the GCC185 binding reaction. The affinities of C-110 for Rab6-GTP and Rab9-GTP are 2.3 ± 0.3 μM SD and 4.5 ± 1.2 μM SD, respectively, with equimolar stoichiometry. Since GST-C-110 is dimeric as determined by gel filtration in conjunction with multiple angle light scattering (data not shown), we conclude that the Rab6/Rab9:C-110 complexes have 2:2 stoichiometry in solution.

Characterization of the Rab-Binding Domain of GCC185

Structure prediction of the GCC185 C terminus using the Paircoil algorithm (Berger et al., 1995) revealed a short dimeric, coiled coil that precisely spans the Rab-binding domain (shaded area, Figure 2A). This region and the GRIP domain were free of predicted unstructured loops (Linding et al., 2003; Figure 2A). In addition, flexible regions were detected downstream of the GRIP domain (~20 residues), and spanning ~40 residues upstream of residue 1527 (Figure 2A).

The RBD-87 Rab-binding domain-containing polypeptide (Figure 1A and top of Figure 2A) was predicted to be ~33% helical by the coiled-coil prediction algorithm. The α-helix content of the RBD-87 polypeptide was determined by circular dichroism to be 40% (Figure 2B). Gel filtration coupled to direct mass measurement by multiple angle static light scattering showed that untagged RBD-87 eluted in a single peak, with a mass of 21.9 kDa, and is therefore a dimer (Figure 2C). Consistent with this finding, chemical crosslinking of RBD-87 yielded efficient conversion to a dimer in solution (Figure 2D). Full-length

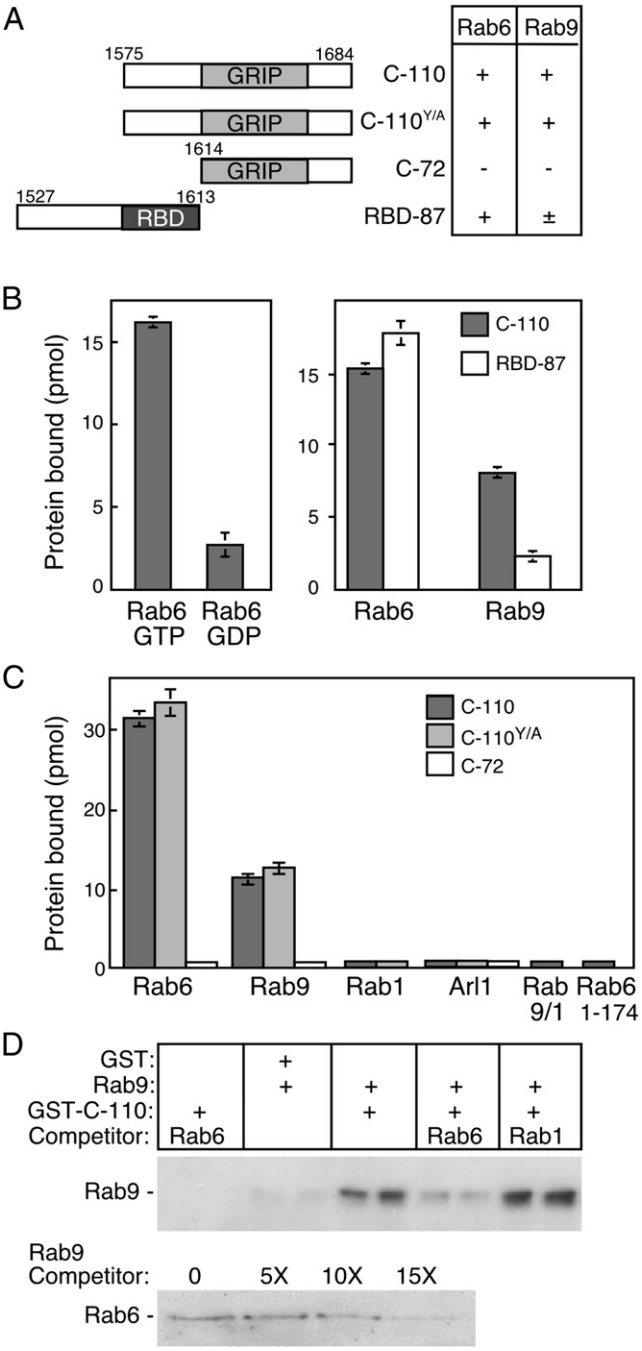

Figure 1. Identification of a GCC185 Rab-Binding Domain

(A) Constructs used to map Rab-GCC185 interactions; numbers represent amino acid residues. The GRIP domain and a Rab-binding domain (RBD) are shown. At right: summary of binding to Rab6 or Rab9.

(B) GCC185 preferentially binds Rab6-GTP via residues upstream of the GRIP domain. Reactions contained 50 pmol His-Rab6 (left) or 1.2 nmol His-Rab6, or Rab9-His (right) using ^{35}S-GTPγS or ^{3}H-GDP-preloaded GTPase and either GST-C110 or GST-RBD-87 (2.8 μM).

(C) The GRIP domain is not sufficient for Rab binding. GST-C-110, C-110$^{Y/A}$, or C-72 (2 μM) was incubated with ^{35}S-GTPγS-preloaded GTPases (~500 pmol) (as in [B] except untagged Rab1, Rab9, Rab9/1, or Arl1Q71L-His or His-Rab6 1–174 were employed).

(D) Rab6 specifically competes with Rab9 for GCC185 binding. GST-C-110:Rab9 complexes (pair of lanes in the center) were incubated for 3 min with ten fold excess competitor. Rab9-His was detected by immunoblot using a monoclonal anti-Rab9 antibody that did not cross react with Rab6 (see pair of lanes at far left). Lower panel, same as upper panel using indicated amounts of competitor Rab9.

Data are mean ± SD.

GCC185 is also dimeric (Luke et al., 2005), consistent with the RBD-87 polypeptide forming a helical dimer.

A helical wheel projection of the predicted coiled coil spanning the Rab-binding domain identified the hydrophobic face of an amphipathic helix, with residues at heptad positions 'a' and 'd' expected to reside at the interface of a dimeric coiled coil (Harbury et al., 1993; Figure 3A). Close inspection of the hydrophilic surface revealed two hydrophobic residues (I1588 and L1595), both at heptad position ('c'), that would be solvent-exposed if this model is correct (residues boxed in Figure 3A). Such residues were outstanding candidates to mediate hydrophobic protein-protein interactions.

I1588 and L1595 were therefore mutated to alanine within the C-110 polypeptide; binding of these mutant proteins to Rab6 and Rab9 was then tested. The I1588A mutant bound ~50% less to Rab9 than its wild-type counterpart (Figure 3B). The L1595A mutation abolished Rab9 binding completely; a double mutant was also binding incompetent, as expected. I1588 and L1595 were also critical for Rab6 binding (Figure 3C). The I1588A mutant showed slightly less (14%) binding than the wild-type polypeptide; L1595A was decreased about 50%, and the double mutant was the most severely impaired (88%). Because the double mutant was more impaired than either single mutant, we conclude that both residues contribute to a Rab-binding interface. The lower affinity of Rab9 for the C-110 fragment (Figure S1) may explain why Rab9 is more sensitive to mutations at these positions.

Dimer formation was not disrupted in the RBD-87 I1588A/L1595A protein, as it behaved as a 20.4 kDa, mono-disperse dimer upon gel filtration and multiple angle static light scattering (Figure 3D), nearly identical to wild-type RBD-87 (Figure 2C). In addition, untagged C-110 I1588A/L1595A yielded a circular dichroism spectrum that was indistinguishable from its wild-type counterpart (data not shown), thus the mutant protein did not appear to be misfolded. Together, these data confirm that Rab9 and Rab6 overlap in their interaction with a coiled-coil Rab-binding domain in GCC185.

Structure of Rab6 Bound to the GCC185 Rab-Binding Domain

The complex of human GCC185 (residues 1547-1612) and the constitutively active mutant of Rab6 (Q72L) was crystallized in the presence of GTP and Mg^{2+} (Table 1). The structure was solved by molecular replacement using the crystal structure of GTP-bound Rab6 (Bergbrede et al., 2005; PDB ID 2gil) as the search model. A large portion of the Rab-binding domain of GCC185 was clearly visible in difference electron density maps, allowing unambiguous placement of sidechains at the binding interface (Figure S2). The sidechain register was verified with an anomalous difference Fourier map of selenomethionine

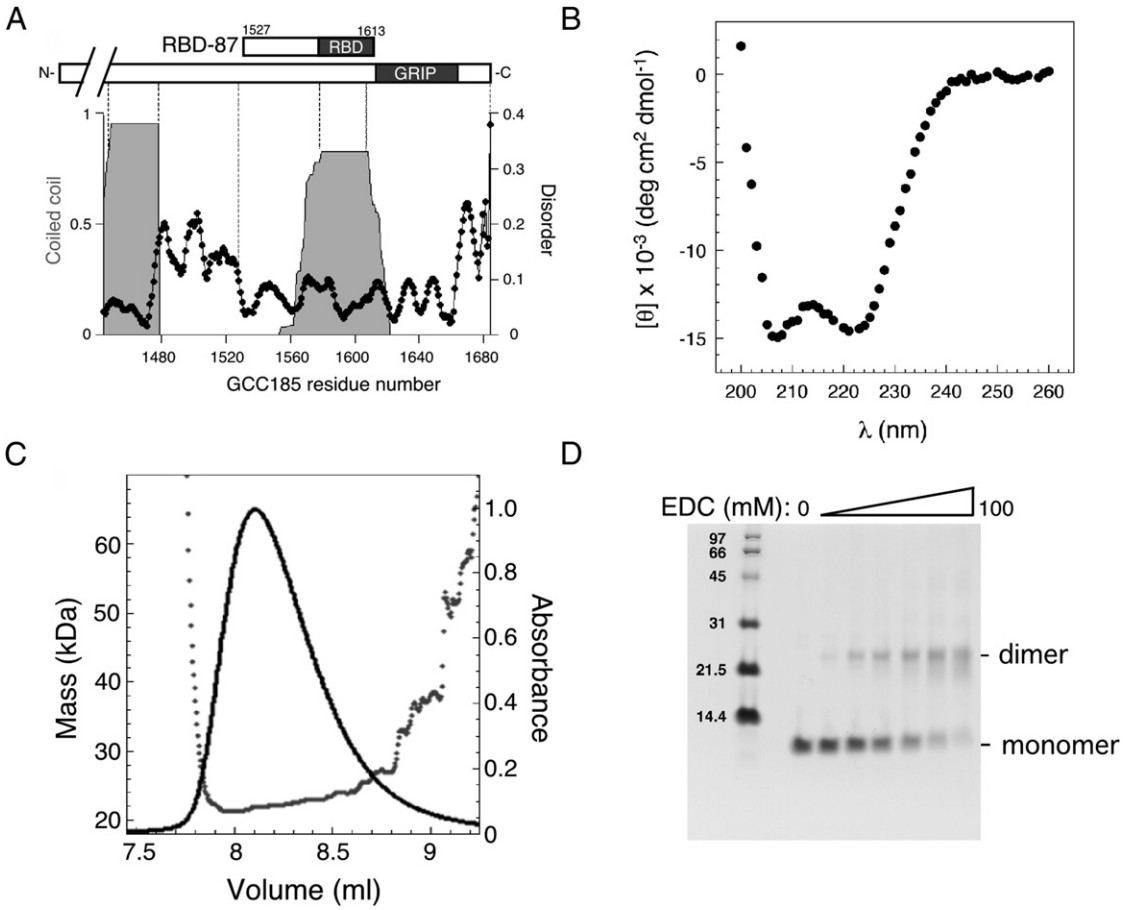

Figure 2. The GCC185 Rab-Binding Domain Is a Helical Dimer

(A) Structure prediction of the GCC185 C terminus. Coiled-coil (shaded gray; cutoff = 0.8) and disordered regions (black line and dots; cutoff = 0.12) in GCC185 residues 1444–1684 were predicted with Paircoil and the DisEMBL programs, respectively. At top: bar diagram of the GCC185 C terminus.

(B) Circular dichroism spectrum of untagged RBD-87 (mean residue ellipticity).

(C) Untagged RBD-87 forms a dimer in solution. Black line, A_{280}. The mass of RBD-87 at different elution volumes was calculated from multiple angle static light scattering data (dots). The polydispersity of the peak was 1.024. The mass of RBD-87 (92 aa) monomer is 10.3 kDa.

(D) Analysis of RBD-87 by crosslinking. Untagged protein (5 μM) was reacted at 20°C for 2 hr with 0–100 mM EDC (1-ethyl-3-[3-dimethylaminopropyl] carbodiimide hydrochloride).

substituted GCC185 in complex with Rab6 (Figure 4B). The final model refined to R_{free} = 26.8 and R = 22.8 at d_{min} = 3 Å (Table 1); it includes Rab6 residues 14–174, GCC185 residues 1570–1607, bound GTP and Mg^{2+}.

Two Rab6-GTP molecules contact the GCC185 coiled-coil dimer with two-fold symmetry (Figures 4A and 4B). Each GCC185 helix bridges two opposing Rab6 molecules (Figure 4B), and conversely, each Rab6 molecule interacts with both helices that comprise the coiled coil. This strongly suggests that Rab binding will stabilize a dimeric GCC185 structure. Extensive contacts comprise a buried interface of 1250 $Å^2$ for a single Rab6 with the GCC185 dimer. For comparison, a similar area is buried in the single Arl1:GRIP dimer interface (PDB ID 1UPT; 1310 $Å^2$; our calculations).

As expected from the nucleotide dependence of Rab interaction (Figure 1), the Rab-binding interface is contributed by switch I and II regions (Figure 4) whose different conformations in the GDP and GTP bound forms primarily reflect the state of the GTPase on its surface (Stroupe and Brunger, 2000). Gratifyingly, the two GCC185 hydrophobic residues required for Rab binding (I1588 and L1595, Figure 3) are part of the interface between Rab6 and the GCC185 Rab-binding domain (Figure 4B, bold; Figure S3). Moreover, two of the three invariant, hydrophobic triad residues of Rabs (F50, W67, and Y82) proposed to be important for Rab:effector interactions (Merithew et al., 2001) interact directly with I1588 (Figure S3), and the third residue also contacts GCC185.

No major conformational changes of Rab6 are observed upon binding to GCC185; Rab6-GTP (Bergbrede et al., 2005; PDB ID 2gil) superimposes with Rab6 in our complex with a root-mean-square deviation (rmsd) of 0.55 Å. This is in contrast to the complexes of Rab11:FIP3 (Eathiraj et al., 2006) and Sec4p:Sec2p (Dong, et al., 2007) where Rab binding to the coiled-coil domains induces major conformational changes in the Rabs.

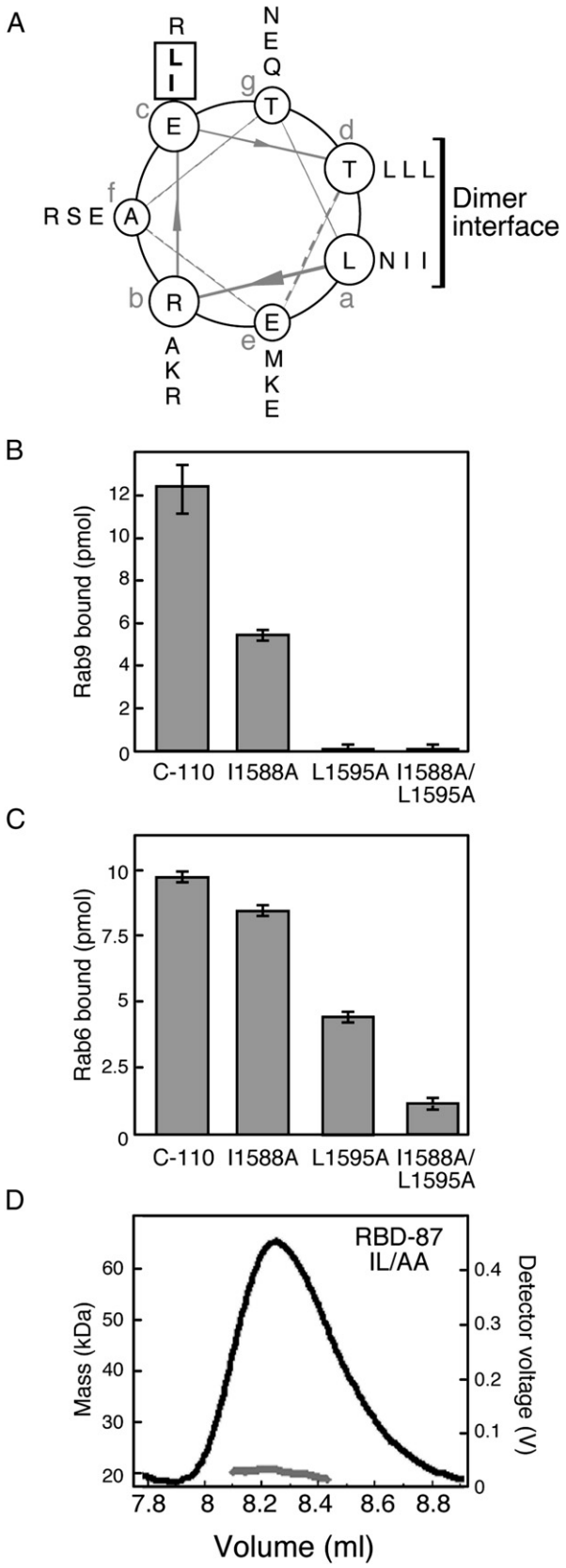

Residues Important for Rab Binding to Regulate Golgi Localization via Rab6

To explore the importance of Rab-binding determinants in GCC185 localization, we expressed wild-type or I1588A/L1595A, C-110 proteins in cultured cells and monitored their localization. Myc-tagged, wild-type C-110 was localized to the Golgi complex as determined by its co-localization with Rab6 protein by confocal microscopy (Figures 5A and 5D). In contrast, the C-110 I1588A/L1595A protein that did not bind Rab6 or Rab9 in vitro (Figures 3B and 3C) failed to localize to the Golgi complex (Figures 5A and 5D). As expected, exogenously expressed, full-length GCC185 was Golgi localized (Figure 5A, top far-right); in contrast, full-length GCC185 containing the I1588A/L1595A substitutions was not (Figure 5A, bottom far-right).

The requirement for residues I1588 and L1595 in Golgi localization showed that Rab-binding domain-determinants dominate the Golgi association process. Consistent with this, a myc-tagged fragment ("C-82") comprised of the 82 C-terminal-most residues of GCC185 (and lacking I1588 and L1595) also failed to associate with the Golgi complex (Figure 5B middle panel), in contrast to C-110 under identical conditions (Figure 5B, left). All transfected cells counted (n = 100) displayed these phenotypes. This differs from a report of Luke et al. (2003) who showed Golgi localization of a similar, GFP-tagged construct. The two studies likely differ because of expression levels (see below).

As shown in Figure 5C, loss of Rab6 (but not Rab9) using siRNA abolished the Golgi localization of the wild-type C-110 fragment. Quantitation showed that > 80% of depleted cells displayed this phenotype (Figure 5D). These data demonstrate that Rab6 is important for Golgi association of GCC185.

Although not sufficient, the GRIP domain in C-82 could still participate in Golgi association. Thus, we tested localization of C-110 Y1618A, which is predicted to not bind Arl1. C-110 Y1618A was less concentrated on the Golgi than wild-type C110 (Figure 5B, right), suggesting that the GRIP domain also contributes to Golgi localization. Indeed, siRNA depletion of Arl1 confirmed a requirement for this GTPase in C-110 localization in living cells (Figure 5C). As expected, Golgin-97 and Golgin-245 also lost Golgi association in Arl1 depleted cells (Figure S4), however global TGN organization remained intact as determined by TGN46 localization (Figure S4). Yet the Y1618A mutation did not completely abolish Golgi localization, from which we conclude that C-110 associates predominantly via Rab-binding domain interactions.

Figure 3. Accessible Hydrophobic Residues in the Predicted Coiled Coil Are Critical for Rab Binding

(A) Helical wheel projection of a coiled coil predicted for GCC185 residues 1579–1606. Residues in registers "a–g" were predicted by the Paircoil program. Residues at positions "a" and "d" lie in the dimer interface. Boxed residues are candidates for binding interactions with Rab GTPases.

(B and C) Effect of alanine substitutions on Rab binding. Reactions contained wild-type or mutant GST-C-110 ([B] 3 μM, [C] 2 μM) and ^{35}S-GTPγS-preloaded GTPases ([B] 170 pmol Rab9-His, [C] 190 pmol His-Rab6). Data are mean ± SD.

(D) Mass determination of untagged RBD-87 I1588A/L1595A by multiple angle static light scattering. The gel filtration elution profile of the protein (black line) and molecular mass (gray line) are shown. Polydispersity of the peak was 1.001.

Table 1. Data Collection and Refinement Statistics

	Native (PDB ID 3BBP)	Seleno-Methionine
Data Collection		
Space group	$P6_422$	$P6_422$
Unit Cell		
a (Å)	168.6	167.4
c (Å)	169.0	167.6
Stoichiometry in asymmetric unit	3 Rab6:3 GCC185	3 Rab6:3 GCC185
X-ray source	SSRL beamline 7-1	SSRL beamline 11-1
Detector	ADSC Q315	Marmosaic 325
Wavelength (Å)	0.9785	0.9791
Resolution range (Å)	50–3.0	50–3.4
d_{min} ($I/\sigma >= 2$[Å])	3.2	3.6
Completeness (%)	99.7	99.9
R_{merge} (%)	25.0	22.6
I/σ (highest resolution shell)	10.1 (0.5)	10.3 (0.8)
Refinement Statistics		
R_{work}/R_{free} (%)	22.8/26.8	
Rmsd bond length (Å)	0.003	
Rmsd bond angles (°)	0.46	
NCS rmsd (Å, Rab6)	0.36	
NCS rmsd (Å, GCC185)	0.5	
% residues in Ramachandran:		
Most favored region	90.7	
Additionally allowed	8.7	
Generously allowed	0.7	
Disallowed	0	
Crystallization		
Method	Vapor diffusion at 20°C. Protein and reservoir solution (1.5 μl each) were mixed and seeded in hanging drops with 0.5 ml reservoir solution.	
Condition	20% (w/v) PEG 3350, 200 mM CNNaS	
Cryoprotection	20% (w/v) PEG 3350, 200 mM CNNaS, 20% (v/v) glycerol, 5 mM HEPES (pH 7.5)	

Rab6 Facilitates Arl1 Binding to GCC185

The localization studies strongly suggested that both Rab-binding and GRIP domains contribute to GCC185 localization. Yet initial binding experiments failed to detect Arl1 binding to the GCC185 GRIP domain (Reddy et al., 2006; Figure 1C). We therefore explored the possibility that Rab association with GCC185 may promote Arl1 binding. Untagged Arl1 GTPase was preloaded with radioactive GTP and desalted to remove unbound nucleotide. Arl1 was then incubated with increasing concentrations of the GST-C-110 fragment, in the presence or absence of Rab6 or Rab9-GTPγS; GST-C-110-bound Arl1 was measured directly in a scintillation counter.

Addition of Rab6 enhanced the ability of GCC185 to bind Arl1 (Figure 6A). In reactions containing < 5 μM C-110 polypeptide, very low levels of Arl1 binding were detected, as shown earlier (Figure 1C; Reddy et al., 2006). For comparison, the GRIP domain of Golgin 245 binds efficiently at 2 μM C-110 (cf. Reddy et al., 2006). When reactions were supplemented with Rab6, Arl1 binding increased up to seven-fold and a sigmoidal, saturable binding profile was observed. This binding profile is suggestive of cooperative binding, consistent with a model in which the binding of the first Arl1 monomer facilitates binding of a second Arl1 monomer to a C-110 dimer. In contrast, addition of Rab9 had a slight inhibitory effect on Arl1 binding (Figure 6A). Rab6-independent binding of Arl1 was only seen at 7 μM GCC185, consistent with the dissociation constant for the Arl1:GCC185 interaction (Kd = 7 μM; Figure S1).

Specificity of Arl1 binding was confirmed by its nucleotide dependence in the presence (Figure 6A) or absence (Figure 6C) of Rab6-GTPγS. It also required the conserved tyrosine residue documented to be important for GRIP domain-Arl1 interactions (Figures 6A and 6B). Arl1 did not bind C-110 Y1618A at concentrations as high as 7 μM mutant protein (Figure 6A, bottom). At this concentration, addition of Rab6 restored ~40% binding of Arl1 protein to C-110 Y1618A, despite the loss of the key tyrosine residue (Figure 6B). This provides independent confirmation that Rab6 can indeed enhance the interaction between Arl1 and GCC185. In summary, our study has revealed a novel and unexpected mechanism by which Rab6 regulates GCC185's ability to bind to Arl1 via its C-terminal GRIP domain.

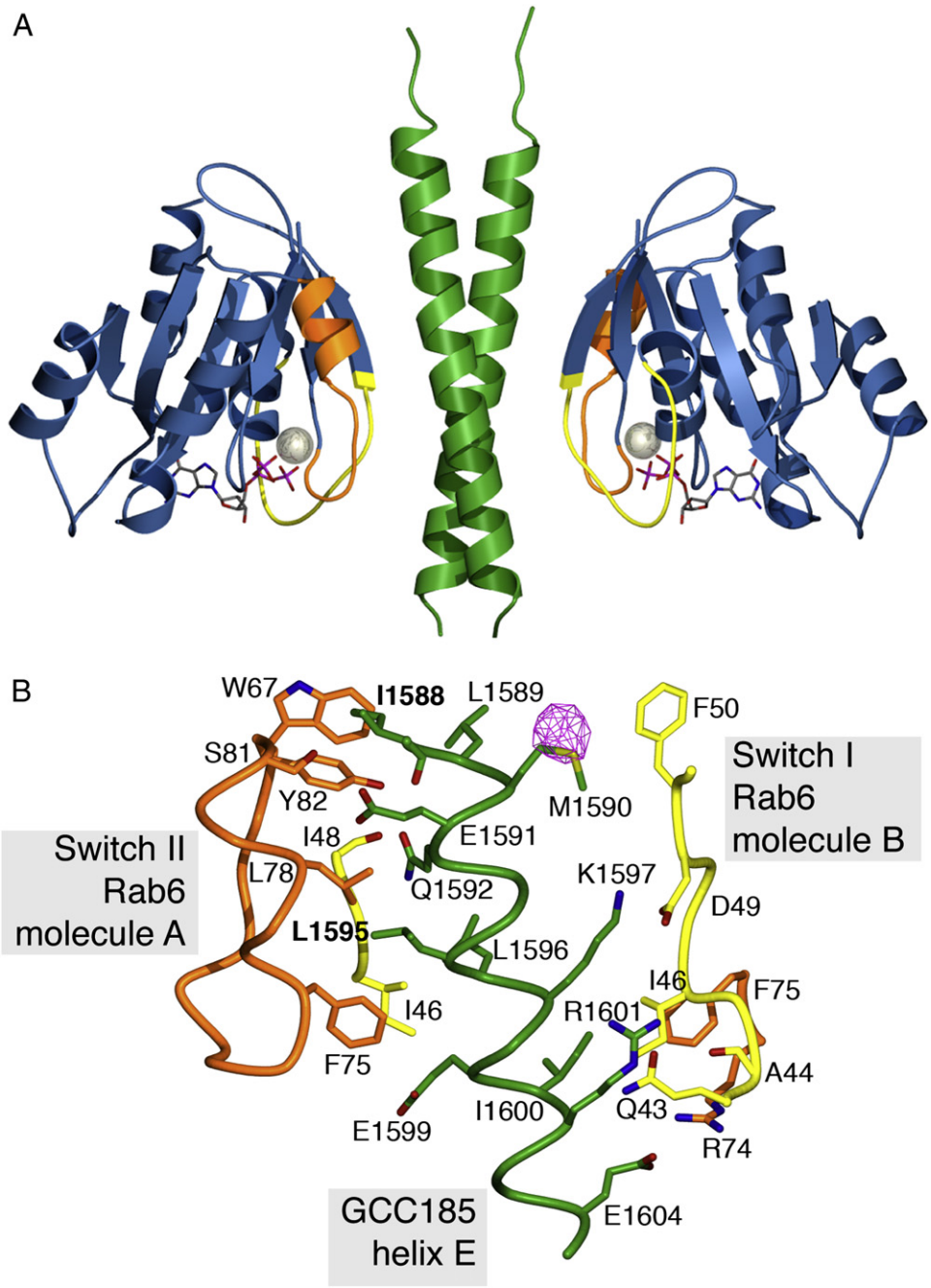

Figure 4. Structure of the Rab6-GCC185 Complex

(A) Ribbon representation of the GCC185 Rab-binding domain dimer (green) and Rab6 (blue) bound to GTP (stick model) and magnesium (sphere). Switch I and II regions of Rab6 (Chattopadhyay et al., 2000) are colored yellow and orange respectively.

(B) View of the Rab6-GCC185-binding interface. A single GCC185 helix (E) out of the two-fold symmetric coiled coil is shown for clarity. Each helix contacts switch regions from two opposed Rab6 molecules A and B. Rab6 switch I and II (including W67) are colored yellow and orange, respectively. Protein backbone (α-carbon trace) and side chains involved in polar and hydrophobic interactions are shown. Carbonyl oxygens are shown for A44, I48, and I1588, and C-Cα bonds have been added to simplify the figure. An anomalous difference Fourier density map of the selenomethionine-substituted crystal (pink, contoured at 6σ) is shown for GCC185.

A Model for Dual GTPase Regulation of GCC185

We used the crystal structure of the dimeric Golgin-245 GRIP domain bound to two Arl1 molecules (Panic et al., 2003) to generate a structure model of the GCC185 GRIP domain bound to Arl1 (see Methods). Simultaneous binding of Rab6 (blue) and Arl1 (gray) to GCC185 was then simulated by combining the Arl1:GRIP

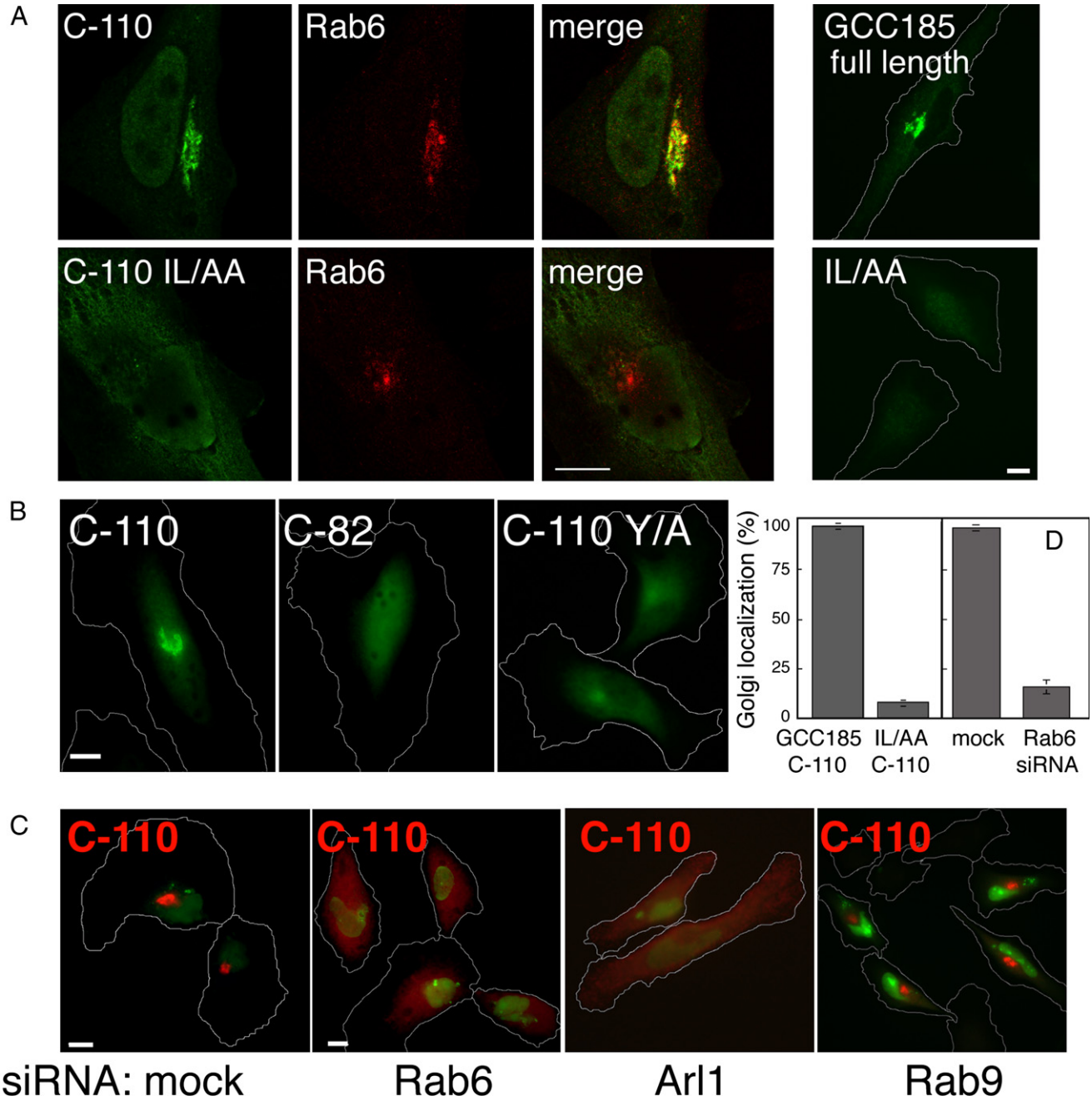

Figure 5. GCC185 Golgi Targeting Requires the Rab-Binding Domain and Rab6 and Arl1 GTPases

(A) Confocal micrograph of HeLa cells expressing myc-tagged wild-type or I1588A/L1595A C-110, 19 hr posttransfection. c-*myc* epitope (green) and Rab6 (red) are shown. A confocal section is shown; image step size was 15.2 nm. Far-right panels were analyzed as in (B).

(B) Conventional fluorescence micrograph of HeLa cells transfected with myc-C-110, myc-C-82 (20 hr posttransfection) or myc-C-110 Y1618A (29 hr posttransfection). Cells were stained as in (A).

(C) Conventional immunofluorescence micrograph of HeLa cells transfected with 6-FAM-conjugated RNA oligonucleotides (green, mock) or these plus siRNAs targeting Rab6, Arl1 or Rab9 as indicated. Postdepletion, and 17 hr prior to fixation, cells were transfected with myc-GCC185 C-110 (red). siRNA-transfected cells are indicated by nuclear green fluorescence from 6-FAM conjugated RNA oligonucleotides.

(D) Quantification of panels (A) and part of (C). Perinuclear myc-fluorescence above background that overlapped with Rab6 staining was scored as Golgi localization. Standard deviations are from two experiments, 100 cells counted per bar shown.

For quantitation of (C), perinuclear fluorescence above background was scored in mock (n = 159 and 113) and Rab6 siRNA- (n = 314 and 210) treated cells in duplicate experiments. The scale bars represent 10 μm.

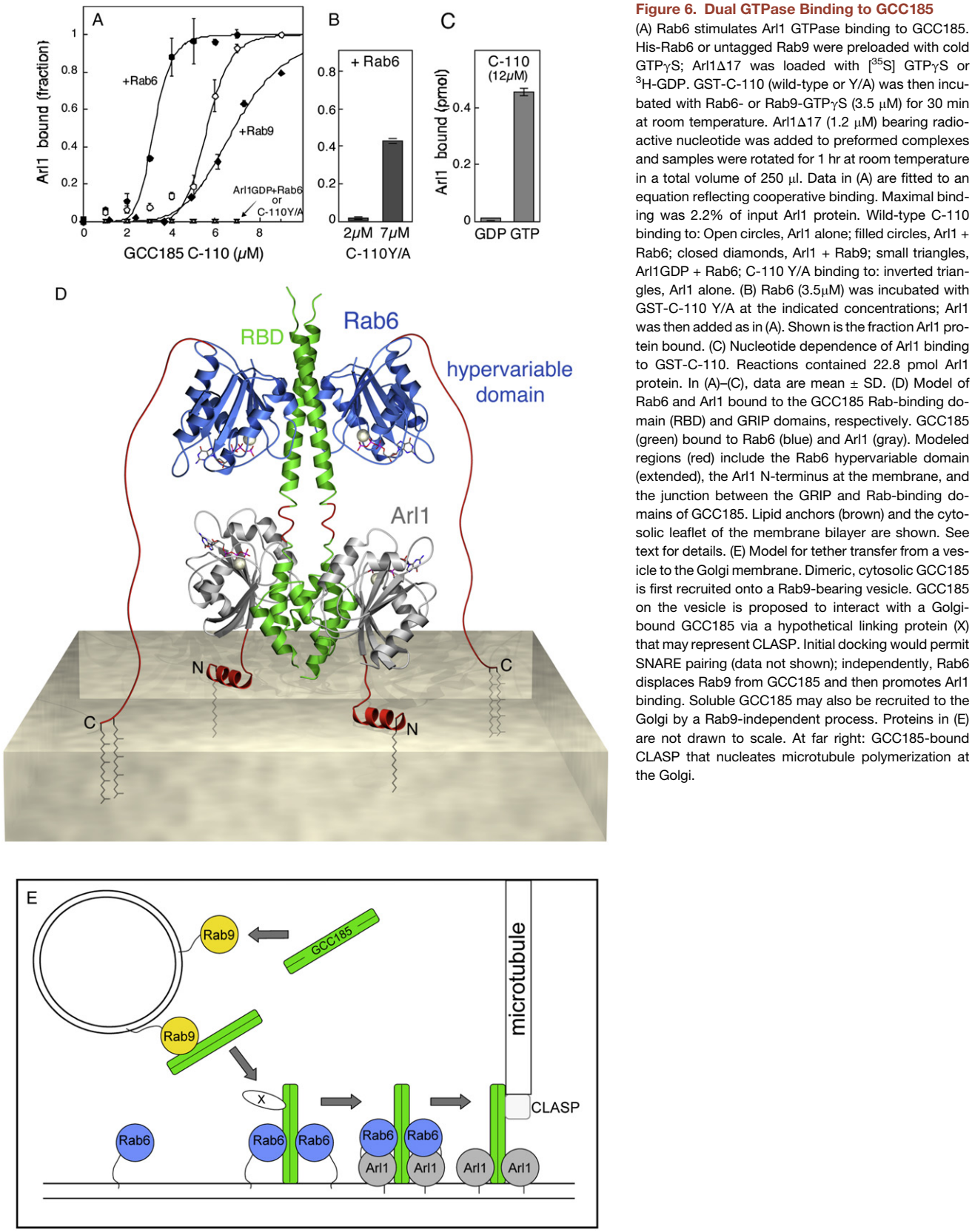

Figure 6. Dual GTPase Binding to GCC185

(A) Rab6 stimulates Arl1 GTPase binding to GCC185. His-Rab6 or untagged Rab9 were preloaded with cold GTPγS; Arl1Δ17 was loaded with [^{35}S] GTPγS or ^{3}H-GDP. GST-C-110 (wild-type or Y/A) was then incubated with Rab6- or Rab9-GTPγS (3.5 μM) for 30 min at room temperature. Arl1Δ17 (1.2 μM) bearing radioactive nucleotide was added to preformed complexes and samples were rotated for 1 hr at room temperature in a total volume of 250 μl. Data in (A) are fitted to an equation reflecting cooperative binding. Maximal binding was 2.2% of input Arl1 protein. Wild-type C-110 binding to: Open circles, Arl1 alone; filled circles, Arl1 + Rab6; closed diamonds, Arl1 + Rab9; small triangles, Arl1GDP + Rab6; C-110 Y/A binding to: inverted triangles, Arl1 alone. (B) Rab6 (3.5μM) was incubated with GST-C-110 Y/A at the indicated concentrations; Arl1 was then added as in (A). Shown is the fraction Arl1 protein bound. (C) Nucleotide dependence of Arl1 binding to GST-C-110. Reactions contained 22.8 pmol Arl1 protein. In (A)–(C), data are mean ± SD. (D) Model of Rab6 and Arl1 bound to the GCC185 Rab-binding domain (RBD) and GRIP domains, respectively. GCC185 (green) bound to Rab6 (blue) and Arl1 (gray). Modeled regions (red) include the Rab6 hypervariable domain (extended), the Arl1 N-terminus at the membrane, and the junction between the GRIP and Rab-binding domains of GCC185. Lipid anchors (brown) and the cytosolic leaflet of the membrane bilayer are shown. See text for details. (E) Model for tether transfer from a vesicle to the Golgi membrane. Dimeric, cytosolic GCC185 is first recruited onto a Rab9-bearing vesicle. GCC185 on the vesicle is proposed to interact with a Golgi-bound GCC185 via a hypothetical linking protein (X) that may represent CLASP. Initial docking would permit SNARE pairing (data not shown); independently, Rab6 displaces Rab9 from GCC185 and then promotes Arl1 binding. Soluble GCC185 may also be recruited to the Golgi by a Rab9-independent process. Proteins in (E) are not drawn to scale. At far right: GCC185-bound CLASP that nucleates microtubule polymerization at the Golgi.

modeled complex with our Rab6:GCC185 Rab-binding domain structure (Figure 6D). The modeled GCC185 GRIP domain was linked to the Rab-binding domain by addition of the only four residues that were not present in either of the two combined structures (red; Figure 6D) to form a continuous helical junction between the GRIP N-termini and the Rab-binding domain coiled coil. Analysis of this junction shows that the two domains cannot be linked by a continuous coiled coil, which implies that this junction may be flexible or even disordered.

Several features of this model are especially noteworthy. The C termini of the Rab6 core domains (blue) face away from the membrane surface and are connected to the 34 amino acid long, Rab6 hypervariable domains (red) which are not visible in our crystal structure. Our model positions Rab6 at the farthest possible distance (up to ~105 Å) from the membrane surface. Nevertheless, the Rab6 hypervariable domain is long enough to accommodate membrane anchoring by two C-terminal prenyl groups. Moreover, this conformation allows insertion of both Arl1 N-terminal helices and myristoyl groups into the membrane (as proposed by Panic et al., 2003; Wu et al., 2004) along an axis that is perpendicular to that of the Rab6 prenyl insertions. Together, the hetero-hexameric complex would form a stable platform to support GCC185 on the membrane with six lipid anchors and two protein helices distributed over four radial attachment points. The GCC185 C-terminal tail may also be inserted in the membrane, further stabilizing the lipid association (Panic et al., 2003). The upright orientation of GCC185 could be important for its role in connecting the TGN to noncentrosomal microtubule tracks (Efimov et al., 2007) and also for its putative function as a tether for transport vesicles.

In summary, the presence of two adjacent GTPase-binding sites suggests an unexpected interplay between these proteins in mediating GCC185 localization and function. A striking aspect of our model is the potential ability of extended Rab hypervariable domains to reach a considerable distance away from the membrane surface where the GTPase catalytic domain contacts and regulates important binding partners.

DISCUSSION

We have shown here that the GCC185 C terminus contains a Rab GTPase-binding site located just upstream of its GRIP domain. Binding of Rab6 to this site promotes association of Arl1 with the GRIP domain, and both GTPases act in concert to localize GCC185 to the TGN. Our structure-derived model of simultaneous GTPase binding offers two possibilities for how these proteins may cooperate. It is possible that the Rab-binding and GRIP domains are conformationally flexible, such that the GRIP domain interacts better with Arl1 upon Rab6 binding. Alternatively, the GTPase pairs may be aligned to allow direct contacts between Rab6 and Arl1. In both cases, stabilization of the coiled-coil dimer by Rab6 may facilitate the dimerization of the GRIP domain, a requirement for Arl1 binding.

A number of proteins rely on bipartite interactions to achieve their specific cellular localizations. For example, EEA1 is targeted to early endosomes by interaction with Rab5 and phosphatidylinositol 3-phosphate, and TIP47 binds late endosomes by interaction with Rab9 and mannose 6-phosphate receptor cytoplasmic domains (see Grosshans et al., 2006 for review). However, rather than just localizing GCC185 to the Golgi, Rab6 may regulate how and when GCC185 binds Arl1. Our experiments show that residues I1588 and L1595 that are important for Rab6 interaction are essential for correct localization of full-length GCC185. We favor a model whereby Rab6 binding initiates stable association with the TGN, but could be dispensible after subsequent GCC185 engagement by two Golgi localized, Arl1 molecules.

Cooperation of G proteins has significant precedent in biology. For example, a Rab GTPase cascade acts in Golgi-to-plasma membrane vesicle transport: one Rab (Ypt32) recruits an effector (Sec2) that acts as a guanine nucleotide exchange factor to activate the subsequently acting, Sec4 Rab protein (Ortiz et al., 2002). In protein translocation, the signal recognition particle (SRP) receptor GTPases, SRα and SRβ cooperate in targeting the signal recognition particle:ribosome nacent chain complex to the endoplasmic reticulum (Halic and Beckmann, 2005). In other cases, an effector may bind two GTPases without obvious influence of one on another: for example, Rab11 and Arf5 or Arf6 bind independently to distinct sites on FIP proteins, without enhancing the other GTPase's binding affinity (Hickson et al., 2003). In our case, binding of Rab6 at one site enhances the binding of a second class of small GTPase to a second site.

Cooperation between Rab6 and Arl1 may be conserved across kingdoms. The single GRIP domain containing protein in *Arabidopsis thaliana* (Gilson et al., 2004) contains a conserved putative Rab-binding domain just upstream of its C-terminal GRIP domain. Residues that comprise the GCC185:Rab6-binding interface are conserved in this protein and assume identical, coiled-coil register positions. In analogy to our study, inclusion of the coiled-coil region conferred efficient Golgi localization (Latijnhouwers et al., 2005; Gilson et al., 2004). Like GCC185, the plant GRIP domain protein also requires Arl1-binding for its localization (Latijnhouwers et al., 2005).

An important aspect of our model is the possibility that Rab proteins may reach some distance from the membrane (up to ~10 nm) to bind to an effector protein, due to the unstructured nature of a Rab protein's ~30 residue, membrane anchored, C-terminal hypervariable domain (Ostermeier and Brunger, 1999; Neu et al., 1997). Thus, unlike Arf-family GTPases that are anchored closely to the membrane by N-terminal sequences and often, myristoylation, Rab proteins show a distinct mode of interaction. Gillingham and Munro (2007) have noted that membrane proximity makes Arf GTPases best suited for vesicle coat recruitment and lipid binding and deformation. The difference in the mode by which these two types of GTPases bind effectors enables Rab and Arf-family members to cooperate in their interactions.

Our crystal structure of the Rab6:GCC185 Rab-binding domain revealed two Rab molecules binding a two-fold symmetric coiled coil. This is in contrast to the asymmetric coiled coil observed in the GEF Sec2p that results in only one Sec4p molecule binding to it (Dong et al., 2007; Sato et al., 2007). Two-fold symmetric coiled coils in the Rabaptin5, RILP and FIP3 effectors offer a pair of binding sites for Rab5, Rab7 or Rab11, respectively (Zhu et al., 2004; Wu et al., 2005; Eathiraj et al., 2006; Shiba et al., 2006). Analysis of the sequence immediately upstream of the

GCC88 GRIP domain suggests it will assume a coiled coil that may also be a Rab-binding site. The corresponding regions in Golgin-245 and Golgin-97 are predicted to be disordered and include numerous proline residues, making it impossible for them to assume a Rab-binding domain structurally similar to that in GCC185. Indeed, neither Rab6 (data not shown) nor Rab9 (Reddy et al., 2006) bind the C terminus of Golgin-245. However, these large coiled-coil proteins may contain additional Rab-binding sites elsewhere in their sequences.

A Model for GCC185 in Tethering at the Golgi Complex

GCC185 is likely to play multiple roles at the Golgi complex. The discovery that it is linked via CLASP proteins to the microtubule-based cytoskeleton may enable Golgi-localized GCC185 to provide a direct track to facilitate the delivery of incoming transport vesicles to the TGN. Live cell video microscopy of Rab9-containing transport vesicles confirmed that they arrive at the TGN along cytoskeletal (and likely microtubule-based) tracks (Barbero et al., 2002).

We propose that GCC185 first associates with transport vesicles via Rab9 (Figure 6E; Reddy et al., 2006). Once these vesicles have arrived at the Golgi (and microtubule minus ends), binding of vesicle-bound GCC185 to CLASP proteins might bring the vesicle close to the TGN to allow docking. After subsequent SNARE interaction (not shown), Rab6 on the Golgi could displace Rab9 and trigger Arl1 binding to GCC185, thus transferring GCC185 onto the TGN. In this model, tethering facilitates vesicle access to TGN-localized t-SNAREs that mediate fusion, a process that may be independent of the Rab/Arl1 transfers shown. After fusion, Rab9 is retrieved from the Golgi by GDI, a protein that extracts Rab-GDP from membranes, for return to late endosomes.

Rab9 seems to interfere with GCC185's ability to bind Arl1, thus Rab6 would need to displace Rab9 from GCC185 before Arl1 could bind. Considering these data altogether, GCC185 could be transferred in a directional manner from one membrane compartment to another, through an ordered set of binding interactions. Future experiments will provide additional mechanistic insight into when, where and how GCC185 engages distinct Rab and Arl GTPases to potentially mediate transport vesicle tethering, motility, and microtubule attachment to the TGN.

EXPERIMENTAL PROCEDURES

Plasmids for Protein Expression

Sequences encoding GCC185 residues $^{1527–1684}$ (C-158), $^{1527–1613}$ (RBD-87), and $^{1614–1684}$-His (C-72) were generated by PCR using the parental templates pGST-GCC185$^{1575–1684}$ (C-110) and pHis-GCC185$^{1343–1684}$ (Reddy et al., 2006). PCR products were cloned into pGEX-6T-1. QuickChange mutagenesis was used to generate I1588A and L1595A mutations and His-Rab6 1-174 in pET15B (Stratagene, La Jolla, CA). Rab6Q72L/S180L/C181L and His-Arl1Q71L 14-181 were generated by PCR and cloned into pET47b. Wild-type or mutant C-110 was amplified by PCR and cloned into pcDNA3 containing an N-terminal triple c-*myc* epitope tag to generate myc-C-82, C-110 and C-110 I1588A/L1595A. pGST-GCC185^{Y1618A} was from Reddy et al. (2006).

Protein Expression, Purification, and Crystallization

Recombinant Rab1, Rab5, His-Rab6, His-Rab6 1–174, Rab9, Rab9-His, Rab9/1, Arl1Δ17, and Arl1Q71L-His proteins were purified (Aivazian et al., 2006). Rab9/1 contains Rab9 residues 1–169 followed by Rab1 residues 173–205. pGST-GCC185$^{1527–1684}$, GCC185$^{1527–1684}$, pGST-GCC185$^{1575–1684}$, pGST-GCC185$^{1614–1684}$-His, Rab6 Q72L/S180L/C181L, and Arl1Q71L-His were transformed into *E. coli* BL21(DE3) cells and induced at an OD_{600} of 0.6 with 1 mM IPTG over night at 23°C. pGST-GCC185$^{1527–1613}$ was induced for 3 hr at 30°C. Protein purification was as described (Reddy et al., 2006). Protein was concentrated in Amicon Ultra filter units (5000 MWCO, Millipore). For crystallization, Rab6Q72L$^{sc180–181LL}$ and GCC185$^{1547–1612}$ were lysed by sonication; the clarified supernatant bound to glutathione-Sepharose 4B (Amersham). GST or His tags were removed with PreScission protease (Amersham) on resin and gel filtered on Superdex 75 16/60 in buffer A (200 mM NaCl, 20 mM HEPES [pH 7.4], 1 mM $MgCl_2$, 0.5 mM DTT). Rab6Q72L$^{sc180–181LL}$ was loaded with 1 mM GTP overnight at 4°C in buffer A. Equimolar Rab6Q72L$^{sc180–181LL}$ (13 mg/ml) and GCC185$^{1547–1612}$ (7.5 mg/ml) (1 ml) were incubated overnight at 4°C in buffer A, 1 mM GTP. The complex was purified on Superdex 75 16/60 equilibrated with buffer A plus 100 mM NaCl and concentrated to 10 mg/ml. Selenomethionyl GCC185$^{1547–1612}$ was prepared (Doublie, 1997), purified as above with 5 mM β-mercaptoethanol; complex with Rab6Q72L$^{sc180–181LL}$ was formed. Initial crystals formed in sitting drops (200nl) containing a 1:1 (v/v) ratio of protein to reservoir solution (condition 61, PEGs I Suite, QIAGEN; Table 1). Diffraction quality crystals obtained by microseeding in hanging drops were cryoprotected prior to freezing in liquid nitrogen. Circular dichroism, multiple angle static light scattering methods, and microscopy and antibodies are in Supplemental Data.

Diffraction Data Collection and Structure Determination

Diffraction data of GCC185:Rab6 complex crystals were collected at 100K and integrated and scaled using DENZO and SCALEPACK, respectively (Otwinowski and Minor, 1997). Data from a crystal containing selenomethionyl substituted GCC185 in complex with Rab6 were collected at the peak wavelength of 0.9791 Å as determined by a fluorescence scan and processed as above. The structure (PDB ID 3BBP) was solved by molecular replacement (Phaser; McCoy et al., 2005) using Rab6 (PDB ID 2gil) as a search model, stripped of solvent, nucleotide and metal ions. Using the molecular replacement phases, a σ_A-weighted $mF_o - DF_c$ electron density map clearly indicated the presence of the Rab-binding domains of GCC185 and bound nucleotide and magnesium in Rab6. The nucleotide was modeled as GTP based on a triphosphate moiety with a bridging magnesium ion. There are three Rab6 molecules and three GCC185 monomers in the asymmetric unit. Two of these Rab6 molecules interact with a GCC185 dimer forming a 2:2 complex, the third Rab6 along with a GCC185 monomer interact with crystallographic-symmetry related molecules to also form a 2:2 complex. Using a generic poly-alanine coiled coil as a starting point (derived from the crystal structure of GCN4 [Gonzalez et al., 1996; PDB ID 1ZIK]), the backbone of the GCC185 Rab-binding domain coiled coil, residues 1570–1607, was built. Electron density maps allowed unambiguous placement of sidechains (Figure S2). The structures of the two 2:2 complexes are nearly identical (rmsd 0.56 Å). Five percent of the observed data were set aside for cross validation, and an initial simulated annealing refinement was carried out using a maximum likelihood amplitude-based target function (CNS; Brunger et al., 1998), resulting in an R value of 30.0%. Further refinement was carried out in Phenix.refine, interspersed with manual model adjustments in Coot (Emsley and Cowtan, 2004). The final stage of refinement treated each Rab monomer as an independent TLS group and the 3 helical GCC185 segments in the asymmetric unit as an independent TLS group, resulting in a substantial decrease (5%–6%) in both R and R_{free} (Table 1).

Molecular Modeling

GCC185 (residues 1612–1665) and Golgin245 (residues 2171–2221) were manually aligned. The GCC185 GRIP domain structure was modeled in SWISS-MODEL and combined with Arl1 using PDB ID 1UPT (Panic et al., 2003). Target and template structures were identical with the only exception of an insertion of three residues in a loop between GCC185 GRIP domain helix 1 and 2. The Rab6 hypervariable domain (residues 175–208) and the Arl1 N-terminal helix (residues 2–16) were built in Chimera (Pettersen et al., 2004) and Coot using PDB files 2D4Z and 1UPT respectively. The interdomain junction of GCC185 (residues 1608–1611) was modeled in Coot by aligning alpha carbons in a helical arrangement at ~3.8 Å from each other.

Nucleotide Loading and Detection of GTPase Binding to GCC185

GTPases (13–26 μM) were loaded with [^{35}S]GTPγS (MP Biomedicals, Irvine, CA) or [^{3}H]GDP (GE Healthcare) and equimolar cold nucleotide in 20 mM HEPES/KOH (pH7.4), 150 mM KCl, 2 mM EDTA, 1 mM $MgCl_2$ and 0.1 mg/ml BSA 37°C (Rab9: 30 min, 37°C; Rab6 and Rab1: 3 hr, 37°C; Arl1, 3 hr, 30°C; Reddy et al., 2006). Arl1 was loaded for 3 hr at 30°C as above but in 4 mM EDTA. Free nucleotide was removed in a NAP-5 column (GE Healthcare) pre-equilibrated in binding buffer (50 mM HEPES/KOH (pH 7.4), 150 mM KCl, 5 mM $MgCl_2$ and 0.1 mg/ml BSA). GST-GCC185 was incubated with pre-loaded GTPases. Complexes were collected with glutathione resin and washed extensively on a solid support. The specific activity of ^{35}S-GTPγS was determined by scintillation counting and bound Rab protein calculated after determining the input in a filter-binding assay. A low GST background was subtracted.

Competition Assay

Rab proteins were pre-loaded with cold GTPγS as above and nucleotide exchange was stopped with 5 mM $MgCl_2$. Rabs (0.5 μM) were then incubated with GST-GCC185$^{1575–1684}$ (5 μM) for 30 min at 22° in 200 μl binding buffer (50 mM HEPES, 150 mM KCl, 5 mM $MgCl_2$, 10 μg/ml BSA) and then bound to 25 μl of a 50% slurry of glutathione beads for 30 min at 22°C. Excess Rab-GTP competitor was added for 3 min and complexes were pelleted by centrifugation at 3500 rpm for 10 s. The supernatant was removed by aspiration with a needle. Complexes were washed 4 × 400 μl in binding buffer and eluted with 40 mM glutathione.

RNA Interference

siGLO Green fluorescent oligonucleotides (Dharmacon Research Inc.) were pooled with Rab6 (Smartpool), Rab9 (Reddy et al., 2006), or Arl1 oligos (50 nM each, Dharmacon) and transfected into HeLa cells at 30% confluency using Oligofectamine (Invitrogen) according to the manufacturer. The Arl1 siRNA target sequence was: AAGAAGAGCUGAGAAAAGCCA. Cells were fixed (Warren et al., 1984) and analyzed 72 hr posttransfection.

Supplemental Data

Supplemental Data include four figures and can be found with this article online at http://www.cell.com/cgi/content/full/132/2/286/DC1/.

ACKNOWLEDGMENTS

This research was funded by grants from the National Institutes of Health (DK37332) to S.R.P. and the Howard Hughes Medical Institute to A.T.B. We thank Drs. D. Aivazian for Rab9/1 binding data, L. Serrano for untagged Rab purification, R. Kahn for Arl1 plasmids, and W. Weis and H. Choi for expertise. A.S.B. thanks Drs. A. Ghabrial and S. Sambashivan for comments on the manuscript.

Received: August 15, 2007
Revised: October 31, 2007
Accepted: November 26, 2007
Published: January 24, 2008

REFERENCES

Aivazian, D., Serrano, R.L., and Pfeffer, S. (2006). TIP47 is a key effector for Rab9 localization. J. Cell Biol. *173*, 917–926.

Barbero, P., Bittova, L., and Pfeffer, S.R. (2002). Visualization of Rab9-mediated vesicle transport from endosomes to the trans-Golgi in living cells. J. Cell Biol. *156*, 511–518.

Barr, F.A. (1999). A novel Rab6-interacting domain defines a family of Golgi-targeted coiled-coil proteins. Curr. Biol. *9*, 381–384.

Bergbrede, T., Pylypenko, O., Rak, A., and Alexandrov, A. (2005). Structure of the extremely slow GTPase Rab6A in the GTP bound form at 1.8 resolution. J. Struct. Biol. *152*, 235–238.

Berger, B., Wilson, D.B., Wolf, E., Tonchev, T., Milla, M., and Kim, P.S. (1995). Predicting coiled coils by use of pairwise residue correlations. Proc. Natl. Acad. Sci. USA *92*, 8259–8263.

Brunger, A.T., Adams, P.D., Clore, G.M., DeLano, W.L., Gros, P., Grosse-Kunstleve, R.W., Jiang, J.S., Kuszewski, J., Nilges, M., Pannu, N.S., et al. (1998). Crystallography & NMR system: a new software suite for macromolecular structure determination. Acta Crystallogr D Biol Crystallogr. *54*, 905–921.

Chattopadhyay, D., Langsley, G., Carson, M., Recacha, R., DeLucas, L., and Smith, C. (2000). Structure of the nucleotide-binding domain of Plasmodium falciparum rab6 in the GDP-bound form. Acta Crystallogr D Biol Crystallogr. *56*, 937–944.

Derby, M.C., van Vliet, C., Brown, D., Luke, M.R., Lu, L., Hong, W., Stow, J.L., and Gleeson, P.A. (2004). Mammalian GRIP domain proteins differ in their membrane binding properties and are recruited to distinct domains of the TGN. J. Cell Sci. *117*, 5865–5874.

Derby, M.C., Lieu, Z.Z., Brown, D., Stow, J.L., Goud, B., and Gleeson, P.A. (2007). The trans-Golgi network Golgin, GCC185, is required for endosome-to-Golgi transport and maintenance of Golgi structure. Traffic *8*, 758–773.

Dong, G., Medkova, M., Novick, P., and Reinisch, K.M. (2007). A catalytic coiled-coil: structural insights into the activation of the Rab GTPase Sec4 by Sec2p. Mol. Cell *25*, 455–462.

Doublie, S. (1997). Preparation of selenomethionyl proteins for phase determination. Methods Enzymol. *276*, 523–530.

Eathiraj, S., Mishra, A., Prekeris, R., and Lambright, D.G. (2006). Structural basis for Rab11-medated recruitment of FIP3 to recycling endosomes. J. Mol. Biol. *364*, 121–135.

Efimov, A., Kharitonov, A., Efimova, N., Loncarek, J., Miller, P.M., Andreyeva, N., Gleeson, P., Galjart, N., Maia, A.R., McLeod, I.X., et al. (2007). Asymmetric CLASP-dependent nucleation of noncentrosomal microtubules at the trans-Golgi network. Dev. Cell *12*, 917–930.

Emsley, P., and Cowtan, K. (2004). Coot: model-building tools for molecular graphics. Acta Crystallogr D Biol Crystallogr. *60*, 2126–2132.

Fridmann-Sirkis, Y., Siniossoglou, S., and Pelham, H.R. (2004). TMF is a golgin that binds Rab6 and influences Golgi morphology. BMC Cell Biol. *5*, 18.

Gillingham, A.K., and Munro, S. (2007). The small G proteins of the Arf family and their regulators. Annu. Rev. Cell Dev. Biol. *23*, 579–611.

Gilson, P.R., Vergara, C.E., Kjer-Nielsen, L., Teasdale, R.D., Bacic, A., and Gleeson, P.A. (2004). Identification of a Golgi-localised GRIP domain protein from Arabidopsis thaliana. Planta *219*, 1050–1056.

Gonzalez, L., Jr., Woolfson, D.N., and Alber, T. (1996). Buried polar residues and structural specificity in the GCN4 leucine zipper. Nat. Struct. Biol. *3*, 1011–1018.

Grosshans, B.L., Ortiz, D., and Novick, P. (2006). Rabs and their effectors: achieving specificity in membrane traffic. Proc. Natl. Acad. Sci. USA *103*, 11821–11827.

Halic, M., and Beckmann, R. (2005). The signal recognition particle and its interactions during protein targeting. Curr. Opin. Struct. Biol. *15*, 116–125.

Harbury, P.B., Zhang, T., Kim, P.S., and Alber, T. (1993). A switch between two-, three-, and four-stranded coiled coils in GCN4 leucine zipper mutants. Science *262*, 1401–1407.

Hickson, G.R., Matheson, J., Riggs, B., Maier, V.H., Fielding, A.B., Prekeris, R., Sullivan, W., Barr, F.A., and Gould, G.W. (2003). Arfophilins are dual Arf/Rab 11 binding proteins that regulate recycling endosome distribution and are related to Drosophila nuclear fallout. Mol. Biol. Cell *14*, 2908–2920.

Kjer-Nielsen, L., Teasdale, R.D., van Vliet, C., and Gleeson, P.A. (1999). A novel Golgi-localisation domain shared by a class of coiled-coil peripheral membrane proteins. Curr. Biol. *9*, 385–388.

Latijnhouwers, M., Hawes, C., Carvalho, C., Oparka, K., Gillingham, A.K., and Boevink, P. (2005). An Arabidopsis GRIP domain protein locates to the trans-Golgi and binds the small GTPase ARL1. Plant J. *44*, 459–470.

Li, B., and Warner, J.R. (1996). Mutation of the Rab6 homologue of *Saccharomyces cerevisiae, YPT6*, inhibits both early Golgi function and ribosome biosynthesis. J. Biol. Chem. *271*, 16813–16819.

Linding, R., Jensen, L.J., Diella, F., Bork, P., Gibson, T.J., and Russell, R.B. (2003). Protein disorder prediction: implications for structural proteomics. Structure *11*, 1453–1459.

Lu, L., and Hong, W. (2003). Interaction of Arl1-GTP with GRIP Domains Recruits Autoantigens Golgin-97 and Golgin-245/p230 onto the Golgi. Mol. Biol. Cell *14*, 3767–3781.

Luke, M.R., Houghton, F., Perugini, M.A., and Gleeson, P.A. (2005). The trans-Golgi network GRIP-domain proteins form α-helical homodimers. Biochem. J. *388*, 835–841.

Luke, M.R., Kjer-Nielsen, L., Brown, D.L., Stow, J.L., and Gleeson, P.A. (2003). GRIP domain-mediated targeting of two new coiled-coil proteins, GCC88 and GCC185, to subcompartments of the trans-Golgi network. J. Biol. Chem. *278*, 4216–4226.

McCoy, A.J., Grosse-Kunstleve, R.W., Storoni, L.C., and Read, R.J. (2005). Likelihood-enhanced fast translation functions. Acta Crystallogr D Biol Crystallogr. *61*, 458–464.

Merithew, E., Hatherly, S., Dumas, J.J., Lawe, D.C., Heller-Harrison, R., and Lambright, D.G. (2001). Structural plasticity of an invariant hydrophobic triad in the switch regions of Rab GTPases is a determinant of effector recognition. J. Biol. Chem. *276*, 13982–13988.

Neu, M., Brachvogel, V., Oschkinat, H., Zerial, M., and Metcalf, P. (1997). Rab7: NMR and kinetics analysis of intact and C-terminal truncated constructs. Proteins *27*, 204–209.

Ortiz, D., Medkova, M., Walch-Solimena, C., and Novick, P. (2002). Ypt32 recruits the Sec4p guanine nucleotide exchange factor, Sec2p, to secretory vesicles; evidence for a Rab cascade in yeast. J. Cell Biol. *157*, 1005–1015.

Ostermeier, C., and Brunger, A.T. (1999). Structural basis of Rab effector specificity: crystal structure of the small G protein Rab3A complexed with the effector domain of rabphilin–3A. Cell *96*, 363–374.

Otwinowski, Z., and Minor, W. (1997). Processing of X-ray diffraction data collected in oscillation mode. Methods Enzymol. *276*, 307–326.

Panic, B., Perisic, O., Veprintsev, D.B., Williams, R.L., and Munro, S. (2003). Structural basis for Arl1-dependent targeting of homodimeric GRIP domains to the Golgi apparatus. Mol. Cell *12*, 863–874.

Pettersen, E.F., Goddard, T.D., Huang, C.C., Couch, G.S., Greenblatt, D.M., Meng, E.C., and Ferrin, T.E. (2004). UCSF Chimera - A Visualization System for Exploratory Research and Analysis. J. Comput. Chem. *25*, 1605–1612.

Pfeffer, S.R. (1999). Transport-vesicle targeting: tethers before SNAREs. Nat. Cell Biol. *1*, E17–E22.

Reddy, J.V., Burguete, A.S., Sridevi, K., Ganley, I.G., Nottingham, R.M., and Pfeffer, S.R. (2006). A functional role for the GCC185 golgin in mannose 6-phosphate receptor trafficking. Mol. Biol. Cell *17*, 4353–4363.

Sato, Y., Shirakawa, R., Horiuchi, H., Dohmae, N., Fukai, S., and Nureki, O. (2007). Asymmetric coiled-coil structure with Guanine nucleotide exchange activity. Structure *15*, 245–252.

Shiba, T., Koga, H., Shin, H.W., Kawasaki, M., Kato, R., Nakayama, K., and Wakatsuki, S. (2006). Structural basis for Rab11-dependent membrane recruitment of a family of Rab11-interacting protein 3 (FIP3)/Arfophilin-1. Proc. Natl. Acad. Sci. USA *103*, 15416–15421.

Siniossoglou, S., and Pelham, H.R. (2001). An effector of Ypt6p binds the SNARE Tlg1p and mediates selective fusion of vesicles with late Golgi membranes. EMBO J. *20*, 5991–5998.

Stroupe, C., and Brunger, A.T. (2000). Crystal structures of a Rab protein in its inactive and active conformations. J. Mol. Biol. *304*, 585–598.

Sztul, E., and Lupashin, V. (2006). Role of tethering factors in secretory membrane traffic. Am. J. Physiol. Cell Physiol. *290*, C11–C26.

Tsukada, M., and Gallwitz, D. (1996). Isolation and characterization of SYS genes from yeast, multicopy suppressors of the functional loss of the transport GTPase Ypt6p. J. Cell Sci. *109*, 2471–2481.

Warren, G., Davoust, J., and Cockcroft, A. (1984). Recycling of transferrin receptors in A431 cells is inhibited during mitosis. EMBO J. *3*, 2217–2225.

Wu, M., Lu, L., Hong, W., and Song, H. (2004). Structural basis for recruitment of GRIP domain golgin-245 by small GTPase Arl1. Nat. Struct. Mol. Biol. *11*, 86–94.

Wu, M., Wang, T., Loh, E., Hong, W., and Song, H. (2005). Structural basis for recruitment of RILP by small GTPase Rab7. EMBO J. *24*, 1491–1501.

Zhu, G., Zhai, P., Liu, J., Terzyan, S., Li, G., and Zhang, X.C. (2004). Structural basis of Rab5-Rabaptin5 interaction in endocytosis. Nat. Struct. Mol. Biol. *11*, 975–983.

Accession Numbers

The structural coordinates and diffraction data for GCC185 bound to Rab6 have been deposited in the Protein Data Bank under ID code 3BBP.